Using the PDGFß-receptor as a target for anti-fibrotic therapies

Student: Zainab Al-Alyan
Student number: S3337189
Department of Nanomedicine and Drug Targeting
Supervisor: Prof. Dr. Klaas Poelstra
University of Groningen
05 July 2022

Table of Content

1. Abstract ... 3

2. Introduction ... 4

Liver fibrosis ... 4

Hepatic Stellate Cells and Myofibroblasts ... 4

Platelet-derived growth factors ... 5

pPB-HSA ... 6

Macrophages and their M1/M2 configuration ... 7

Interferon gamma and Fibroferon ... 7

Aim of the thesis ... 8

3. Materials and methods ... 9

Cell lines ... 9

Binding of pPB-HSA to PDGFß-receptor in 3T3 fibroblasts in vitro ... 9

Immunocytochemical staining of 3T3 fibroblasts ... 9

Intracellular FACS-staining of collagen I in 3T3 fibroblasts ... 9

Nitric oxide (NO) release bioassay in 264.7 RAW macrophages ... 10

3-[4,5-dimethylthiazole-2-yl]-2,5-diphenyltetrazolium bromide (MTT) assay in 264.7 RAW macrophages ... 10

Quantitative real-time PCR ... 10

4. Results ... 11

Binding of pPB-HSA to the NIH3T3 fibroblasts ... 11

Binding of pPB-HSA and HSA to NIH3T3 fibroblasts ... 12

Specificity of the binding of pPB-HSA to the PDGFß-receptor in NIH3T3 fibroblasts using PDGF-BB ... 13

Specificity of the binding of pPB-HSA to the PDGFß-receptor in NIH3T3 fibroblasts using TGF-β ... 14

Effect of compounds on the PDGFβ-receptor expression ... 15

Intracellular uptake of pPB-HSA in NIH3T3 fibroblasts ... 16

NO and MTT assay in 264.7 RAW macrophages ... 17

Anti-fibrotic effects of IFNγ and Fibroferon in NIH3T3 fibroblasts ... 18

Effect of TGF-β, IFNγ and Fibroferon on the intracellular collagen I in NIH3T3 fibroblasts ... 19

5. Discussion ... 20

Conclusion ... 24

References ... 25

Appendices ... 29

Appendix 1: Protocols ... 29

1.1 Synthesis of Alexa$_{647}$-coupled pPB-HSA and Alexa$_{647}$-coupled HSA ... 29

1.2 Measuring binding of pPB-HSA and other compounds with the FACS ... 29

1.3 Immunocytochemical staining *29*

1.4 Intracellular FACS-staining of collagen I in 3T3 fibroblasts *30*

1.5 Quantitative real-time PCR *31*

1.6 Nitric Oxide assay in 264.7 RAW macrophages *31*

1.7 3-[4,5-dimethylthiazole-2-yl]-2,5-diphenyltetrazolium bromide (MTT) assay in 264.7 RAW macrophages *31*

1. Abstract

Liver fibrosis is a disease characterized by the production of excessive amounts of extracellular matrix (ECM) and collagen I and can be caused by alcohol abuse, genetic disorders, vital infections, or a metabolic syndrome. It can eventually lead to liver cirrhosis and hepatocellular carcinoma causing more than 1 million deaths per year worldwide. Hepatic stellate cells (HSC) play a key role in the development of fibrosis. During liver injury, the cells are activated and will change their morphology into fibrogenic myofibroblasts which are the main cellular drivers of hepatic fibrosis. HSCs can also be further activated by releasing excess amounts of transforming growth factor-beta (TGF- ß) and platelet derived growth factor (PDGF). Not only do HSCs produce PDGF, but they also express the PDGFß-receptor making it a potential target to treat liver fibrosis.

This thesis focusses on using the PDGFß-receptor as a target by using a carrier where albumin is coupled to a PDGFR-ß recognizing cyclic peptide (pPB-HSA) which specifically binds this receptor expressed on NIH3T3 fibroblasts. In vitro experiments were performed by using NIH3T3 fibroblasts and RAW 264.7 macrophages. Interferon gamma (IFNγ) is a pro-inflammatory and anti-fibrotic cytokine which was used to determine anti-fibrotic effects in NIH3T3 cells as well as Fibroferon, which is a peptide that delivers IFNγ to the PDGFß-receptor by coupling the cytokine to the peptide pPB.

The binding was determined by the cytoflex which showed that pPB contributes to the binding since HSA alone did not show any effect. The specificity using PDGF-BB and TGF-ß could not be determined but showed great potential for future experiments. IFNγ showed an increased NO response whereas Fibroferon had no induction of NO production showing potential anti-fibrotic effects.

Altogether, the experiments show great potential in using the PDGFß-receptor as a target for liver fibrosis with the use of the cytoflex.

Keywords: Fibrosis, pPB-HSA, HSCs, PDGFß-receptor, Fibroferon, TGF-β, IFNγ, PDGF-BB.

2. Introduction

Liver fibrosis

Liver fibrosis is a disease that can result after long-term injury to liver cells and is one of the major causes of mortality and morbidity worldwide. It can be caused by alcohol abuse, genetic disorders, viral infections or a metabolic syndrome[1]. One of the other causes is the infection with hepatitis B and C where over the world more than 350 million people are infected with hepatitis B leading to hepatocellular carcinoma and cirrhosis. These diseases lead to approximately 1 million deaths per year worldwide[2]. Until now, no approved therapies are available to treat liver fibrosis. The current treatment of the disease is focused on removing the underlying cause by making lifestyle changes, clearing infections, or taking certain medicine[1,3]. There is rising evidence that the fibrosis is reversible by successfully removing stimuli[4]. The end stage of liver fibrosis is liver cirrhosis which can lead to liver failure and hepatocellular cancer. Liver transplantation is then the only available treatment[1,4]. The main characterization of liver fibrosis and liver cirrhosis is the altered composition of the extracellular matrix (ECM)[1,4,5,6]. This can be used to find potential therapeutic approaches to cure this disease.

Hepatic Stellate Cells and Myofibroblasts

Hepatic stellate cells (HSC) reside in the perisinusoidal space between the space of Disse and hepatocytes and are also called perisinusoidal cells. These cells contribute primarily to fibrogenesis in liver injury[4,5,6]. The main function of HSCs is the storage of vitamin A in lipid droplets[4,5,6]. When there is chronic hepatic disease, quiescent HSCs get activated and they will progressively lose their vitamin A, cause ECM deposition and cellular contraction. They will transdifferentiate and change their morphology into fibrogenic myofibroblasts (MFBs) which are the cellular drivers of hepatic fibrosis[4,5]. They will synthesize large amounts of ECM and collagen fibers and thereby destroying the physiological architecture of the liver[7,8]. HSCs can also migrate to the site of injury where it can upregulate mesenchymal markers (like fibronectin, collagen a1 and a-SMA) and downregulate neural markers that are characteristic for normal, non-activated HSC[4,5]. The cells can also be further activated via paracrine effects by releasing excess amounts of tumor necrosis factor-alpha (TNFα), transforming growth factor-beta (TGF-ß), and platelet derived growth factor (PDGF)[2,6,12].

When there is injury, damage-associated molecular patterns (DAMPs) are released by the HSCs, stimulating the activation of immune cells including Kupffer cells, that will lead to the secretion of pro-fibrotic and pro-inflammatory factors[7,9]. Normally, the regulation between ECM synthesis and degradation is regulated by a balance between tissue inhibitor of metalloproteinase (TIMPs) and matric metalloproteinases (MMPs)[7-9]. MMPs plays a role in the synthesis of ECM proteins while TIMPs can cause degradation of ECM proteins and cause turnover in homeostasis and disease[7-9]. When excess amounts of ECM and collagen are produced, the balance between MMPs and TIMPs is broken causing formation of scar tissue. The structure of the liver tissue will be destructed as well as the physiological function which contributes to the formation of liver fibrosis[7-9].

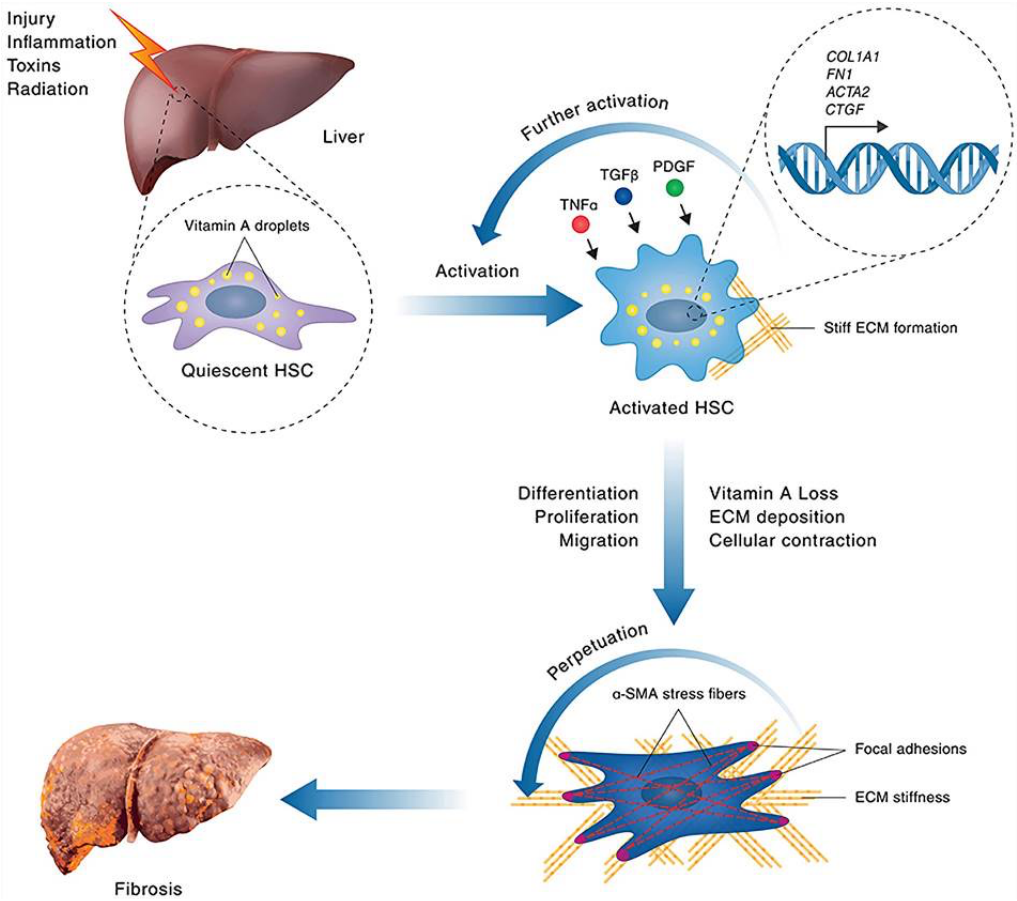

Figure 1: The mechanism of the progression of liver fibrosis. After the liver gets injured, quiescent HSC's will be activated and lose their vitamin A which is stored in lipid droplets. The activated HSC's can be further activated by TNFα, TGFβ and PDGF causing vitamin A loss, ECM deposition and cellular contraction. HSC's change their morphology to myofibroblasts contributing to the development of liver fibrosis by synthesis of extracellular matrix (ECM)[16].

Platelet-derived growth factors

During the development of connective tissue cells, the platelet-derived growth factors (PDGFs) play an important role. They consist of four cysteine-knot-type growth factors (PDGF-A, -B, -C and -D) and are present in a dimeric form, four homodimeric forms (AA, BB, CC and DD), and in one homodimerc form (AB)[10-12]. In liver fibrosis the isoform of PDGF that is the most prominent is PDGF-BB. It is secreted by infiltrating and resident cells of the liver like activated Kupffer cells (M2-dominant type), infiltrating monocytes and macrophages, platelets and hepatocytes which affects the expression of both PDGF and its receptor. The cells that are primarily affected are the myofibroblasts and the HSCs. PDGF can cause the transition of quiescent stellate cells into activated stellate cells causing the production of PDGF-BB which leads to an autocrine profibrotic loop since the myofibroblasts and HSCs, in mice and humans, have a highly induced PDGFß-receptor expression[10,13]. The profibrotic loop is created without the interference of other cells[8]. The four types of PDGF bind to two PDGF receptors, PDGFR-α and PDGFR-ß, with different specificity and affinity. The homodimer PDGF-AB or PDGF-BB binds to both of the receptors whereas PDGF-C only binds to the PDGFR-α. PDGF-D interacts by low affinity with PDGFR-αß but interacts predominantly with homodimeric PDGFR-ß. The activated PDGFR-α and PDGFR-ß have unique signaling outcomes but also trigger overlapping physiological roles [10,12,14,15].

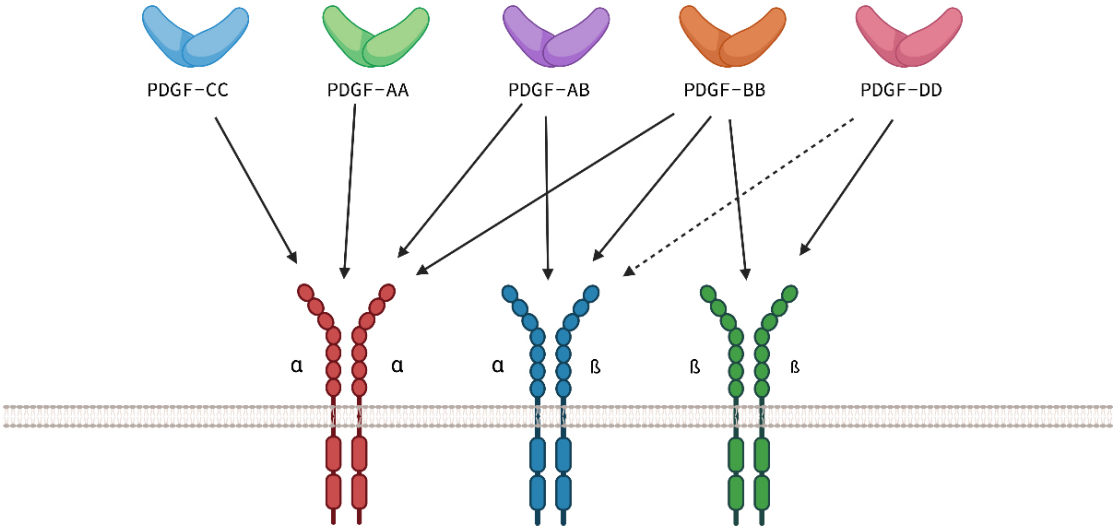

Figure 1: The different PDGF-PDGFR interactions. PDGF-CC binds only to the PDGFRα. PDGF-AA binds to PDGFR-α and PDGFR-αß and PDGF-BB binds to all three of the receptors. PDGF-DD has a low affinity for PDGFR-αß and binds primarily to the PDGFR-ß. https://app.biorender.com/illustrations/61fa767ea30d5d009eb06ac0

The typical function of the PDGFs is the regulation of embryonic development where they especially play a role in the formation of organs and vessels. It also promotes vascular smooth muscle cell migration, wound healing, integrity of the blood brain barrier and interstitial fluid pressure[10,14,16]. In fibrotic livers, the expression of PDGF and its receptor is increased by several fibrotic and inflammatory mediators like TGF-ß, tumor necrosis factor alpha (TNFα) and interleukin-1ß[10]. In addition, liver fibrosis might induce increased intestinal permeability due to the release of many mediators, and this in turn may cause leakage of LPS[10]. This also results in further upregulation of the PDGFR expressions in the liver[10,14]. The expression of the PDGF receptors is enhanced in the fibroblast-like cells but also the production of PDGF is increased which together leads to further development of fibrosis in the liver[15]. This makes HSCs a target for anti-fibrotic therapies in the liver.

pPB-HSA

Just as described before, the PDGFß-receptor expression is upregulated in liver fibrosis making it a great target for therapeutic approaches. That is why a cyclic peptide (pPB) has been designed against PDGFß-receptor. Multiple PDGFβR-recognizing peptide moieties (pPB) were coupled to human serum albumin (HSA) forming a drug carrier protein. This leads to the binding of pPB-HSA to the PDGFβ-receptor without activation of the downstream intracellular signaling pathway[15,17]. The cyclic peptide was coupled to albumin since pPB alone does not displace PDGF-BB from its receptor whereas pPB-HSA does cause a competitive effect[10]. This way, a PDGF receptor-recognizing peptide can be synthesized and used for targeting purposes to deliver anti-fibrotic drugs to the right receptor by minimalizing adverse effects and increasing the efficacy[15,17,18].

Macrophages and their M1/M2 configuration

Macrophages are cells that are widely present in the body and will be activated in presence of internal and external danger signals to provide the first line of defense[19,20]. The main function of the macrophages is to maintain homeostasis throughout life. During damage, the cells will initiate immune responses which leads to the activation of T and B cells to destroy any pathogens in the body[19-21]. This is followed by a recovery phase where the damaged tissue is restored to maintain homeostasis in the body[19,20]. Macrophages can be activated in two different phenotypes, M1 and M2 according to their environment which have complementary and opposing functions in fibrosis[21]. Lipopolysaccharide (LPS) can cause the macrophages to drive to the M1 phenotype whereas the M2 phenotype is induced by interleukin 4 (IL-4), interleukin 10 (IL-10) or TGF-β[19-22]. When cells get infected, the cells will firstly be polarized into the M1 phenotype which gives a pro-inflammatory response to host against pathogens. Subsequently, the cells switch to the anti-inflammatory M2 phenotype to repair any damage that is present in the tissue[19-22].

Nitric oxide (NO) is a gaseous radical and reactive metabolite which is produced by nitric oxide synthase (NOS). During infections, inflammation, and stress, NO and NOS can be detected in macrophages. A major stimulator of the production of NO in macrophages is LPS[23,24]. LPS induces the synthesis of NO in macrophages which plays a role in host defense mechanisms, neurotransmission, and inflammation mechanisms. In excessive amounts, NO can lead to damage in the endothelial tissue[23,24].

Interferon gamma and Fibroferon

Interferon gamma (IFNγ) belongs to the interferons (IFNs) which is part of the interferon/interleukin-10 cytokine family. It is an immunomodulatory cytokine that is secreted and expressed by immune cells (like T cells and mainly natural killer cells) after recognition of infected cells[10,25,26,27]. The role of IFNγ in the liver is regulation of cell cycle progression and hepatocyte apoptosis but it has also been found that it is highly effective in chronic inflammatory diseases, tumors, immunodeficiency diseases, fibrosis and atypical mycobacterial infections[1,26]. It interacts via its IFNγ receptor which leads to the activation of the Jak-STAT1 signaling pathway[17,19]. The production of IFNy on the other hand is amongst others mediated through the Toll-like receptor (TLR), which is the receptor for LPS. The receptor can be activated and trigger the production of IFNγ by lipids, proteins and microbial nucleic acids[28].

IFNγ can have a variety of effects within the liver. The main function of IFNγ is that it activates macrophages by the inducing production of TNFα and interleuking-12. It also stimulates the macrophages to kill phagocytosed microbes and cancer cells[10]. In macrophages, it can upregulate and induce the inflammatory (M1) activation state. This leads to the increase of cytotoxic T cell recognition of foreign peptides but can also promote the differentiation of T- and B-lymphocytes which contributes to the promotion of fibrosis as well as the activation of neutrophils[10,29]. Furthermore, the production of the proinflammatory factors also lead to promotion of fibrosis by activating HSCs to becoming profibrotic myofibroblasts[10]. Next to pro-fibrotic effects, IFNγ can also have direct antifibrotic effects due to direct inhibition of HSC activation by apoptosis and cell cycle arrest. It can inhibit the proliferation of HSCs and decrease the extracellular matrix gene expression contributing to antifibrotic effects[10,26,29].

Although IFNγ has antifibrotic effects, the clinical application is limited due to adverse effects and low efficacy. To minimalize these effects and have a higher efficacy, the cytokine IFNγ was coupled to a cyclic peptide (pPB) to form the peptide Fibroferon. It is an IFNγ-derived mimetic peptide based on the structure of IFNγ and PDGF-BB. It is thereby specifically delivered to activated myofibroblasts and HSC since these cells have a high expression of the PDGFBR[10,30].

Aim of the thesis

The aim of the thesis is to use the PDGFβ-receptor as a target to find a therapy for liver fibrosis. This will be done by testing the binding and specificity of pPB-HSA and examine the anti-fibrotic properties of IFNγ and Fibroferon in vitro. NIH3T3 cells will be used as well as RAW 264.7 cells which represent respectively the mouse fibroblasts and macrophages. The binding of pPB-HSA will be examined by using the Cytoflex which has not been done before. With these experiments, a new way of measuring the binding of pPB-HSA can be discovered to potentially find a therapy for liver fibrosis.

3. Materials and methods

Cell lines

Mouse NIH3T3 cells (fibroblasts) were obtained from the European Collection of Authenticated Cell Cultures (ECACC, UK). The NIH3T3 fibroblasts were cultured in Dulbecco's modified Eagle's medium (DMEM (1X), GlutaMAX™) supplemented with 5ml 10.000 U/ml penicillin and 10,000 µg/ml streptomycin in 500 ml medium, 10% fetal bovine serum (FBS), 2 mM L-glutamine, 4500 mg/L glucose, 1500 mg/L sodium bicarbonate and 1 mM sodium pyruvate. The cells were cultured in T75 flasks at 37˚C with 5% CO_2. The cells were used from passage 172-173+0-25.

RAW 264.7 cells (macrophages) were obtained from The European Collection of Authenticated Cell Cultures (ECACC,UK). The RAW cells were cultured in Dulbecco's modified Eagle's medium (DMEM (1X), GlutaMAX™) supplemented with 120 µl 50 mg/ml Gentamycin in 500 ml medium, 10% fetal bovine serum (FBS), 4 mM L-glutamine, 4500 mg/L glucose, 1500 mg/L sodium bicarbonate and 1 mM sodium pyruvate. The cells were cultured in T75 flasks at 37˚C with 5% CO_2.

Binding of pPB-HSA to PDGFß-receptor in 3T3 fibroblasts in vitro

NIH3T3 cells (50,000 cells/well) were plated in a 24-well culture plate and incubated for 24 hours at 37˚C with 5% CO_2. Subsequently, medium alone and pPB-HSA-$Alexa_{555}$ were added in different dilutions and incubated for 1 hour at 37˚C with 5% CO_2. After 1 hour, the cells were washed, centrifuged and the binding was determined using FACS analysis. In case of measuring the effect of a compound on the binding of pPB-HSA to the cells, the compound was added either 1 or 2 hours prior to the addition of pPB-HSA.

Immunocytochemical staining of 3T3 fibroblasts

NIH3T3 cells (50.000 cells/well) were plated in a 24-well culture plate with sterile plastic cover slips and incubated for 24 hours at 37˚C with 5% CO_2. After 24 hours, medium alone and 5 ng/ml of human recombinant TGFß was added and incubated for another 24 hours. Then the cells were incubated with medium alone, 1µg/ml IFN and 1.35µg/ml Fibroferon for 24 hours. The cells were fixed using methanol:aceton (1:1 ratio), dried and stored at -20˚C. The cells were rehydrated with PBS and incubated with the primary antibody in appropriate dilution for 1 hour at room temperature. Cells were then incubated with the secondary antibody for 30 minutes at room temperature. Following incubation with the tertiary antibody for another 30 minutes at room temperature. The cover slips were washed with PBS and stained with the NovaRed staining kit as per manufacturer's instructions. Subsequently, counterstaining with hematoxylin was performed for 1 minute after washing with demi-water. The slips were washed afterwards with tap-water and were mounted with DEPEX. The cells were visualized using a light microscope.

Intracellular FACS-staining of collagen I in 3T3 fibroblasts

NIH3T3 cells (50,000/well) were plated in a 24-well culture plate and incubated for 24 hours at 37˚C with 5% CO_2. After 24 hours, medium alone and 5 ng/ml of human recombinant TGF-ß was added and incubated for another 24 hours. Then the cells were incubated with medium alone, 1µg/ml IFNγ and 1,35µg/ml Fibroferon for 24 hours. Subsequently, the cells were

transferred to FACS tubes and centrifuged for 5 min by 300 g. The cells were resuspended with Fix/Perm (eBioscience) and incubated for 30 minutes on ice. The cells were then incubated with the primary antibody for 1 hour on ice. After an hour, the cells were centrifuged and vortexed with Perm Buffer (eBioscience) and centrifuged again. The cell pellet was incubated with the second antibody for 30 minutes on ice. After incubation and centrifuging the third antibody was added and the cells were incubated for another 30 minutes on ice. The samples were then measured at the Flow Cytometry (European Research Council).

Nitric oxide (NO) release bioassay in 264.7 RAW macrophages

RAW 264.7 cells (100,000 cells/well) were seeded in a 96-wells plate and incubated for 24 hours at 37˚C with 5% CO_2. After 24 hours, RAW medium alone and the conditioned medium of the different treatments of the extracellular FACS-staining of collagen I in 3T3 cells was added to the RAW cells and incubated at 37˚C with 5% CO_2. After 24 hours, the secreted nitrite was measured with the ThermoMax microplate reader (Molecular devices) with an absorbance at 550 nm. Griess reagent was used (1% sulfanilamide; 0,1% naphthylethylendiamine dihydrochloride, 3% H_3PO_4).

3-[4,5-dimethylthiazole-2-yl]-2,5-diphenyltetrazolium bromide (MTT) assay in 264.7 RAW macrophages

The MTT assay was performed using the same wells plate that was used during the NO assay. 100µl of the samples in the plate was removed and 100µl of Tetrazolium solution (0,5mg/ml in DMEM) was added to each well. The cells were then incubated for 10-60 min at 37˚C. Subsequently, the supernatant was discarded and 100µl of DMSO was added to each well. The plate was then put on a shaker at room temperature until the purple was dissolved after which the absorbance was measured with the ThermoMax microplate reader (Molecular devices) at 550nm.

Quantitative real-time PCR

Total RNA from 3T3 fibroblasts was isolated using the Maxwell simplyRNA kit (Promega) according to Manufacturer's instructions. The RNA concentration was measured on a Nanodrop spectrophotometer (Nanodrop Technologies). Total RNA (~50ng/µl) was reverse transcribed by using the cDNA synthesis kit (Promega) in a volume of 50µl. The primers that were used and the sequences can be found in appendix 1.5. For the quantitative real time PCR analysis, 20ng of cDNA was used. For performing the reactions, SYBR green PCR master mix (Applied Biosystems) was used and performed according to the manufacturer's instructions. The reactions were analyzed by using the detection system. The housekeeping gene b-actin was used to normalize the relative gene expression.

4. Results

Binding of pPB-HSA to the NIH3T3 fibroblasts

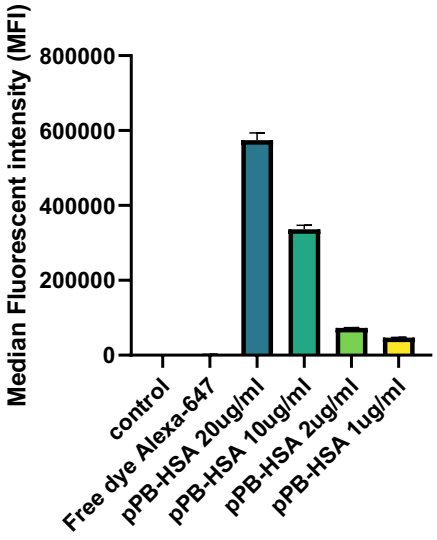

Graph 1: The binding of pPB-HSA to the PDGFβ-receptor in NIH3T3 fibroblasts measured with the cytoflex at a wavelength of 638 nm. pPB-HSA was added in different concentrations (1µg/ml, 2µg/ml, 10µg/ml and 20µg/ml).

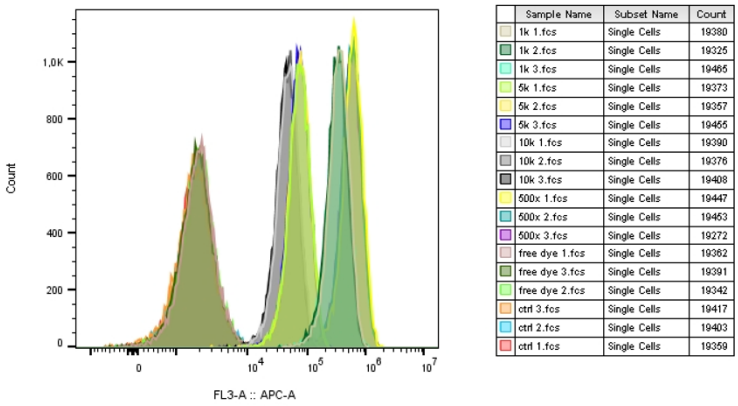

Graph 2: The binding of pPB-HSA to the PDGFβ-receptor in NIH3T3 fibroblasts measured with the cytoflex at a wavelength of 638 nm. pPB-HSA was added in different dilutions (1µg/ml, 2µg/ml, 10µg/ml and 20µg/ml).

To determine the binding of pPB-HSA to the 3T3 cells, pPB-HSA was added in different concentrations and the median fluorescence intensity (MFI) was measured which indicates the binding of the peptide to the 3T3 cells. 50,000 NIH3T3 cells were plated in a 24-wells plate and incubated overnight after which the different concentrations of pPB-HSA were added. The cells were then measured with the cytoflex after an hour of incubation with the pPB-HSA to analyze the binding to the cells.

Graph 1 and graph 2 show the binding of pPB-HSA in different dilutions to the PDGFβ-receptor in 3T3 fibroblasts. Graph 2 shows the graph that has been obtained by the cytoflex. These measurements were done in triplo. Free dye was also added which contained only $Alexa_{647}$ to see whether the dye alone causes binding to these cells. Graph 1 shows that the free dye causes no increase in MFI in comparison with the control indicating no binding or uptake to the cells since the control contains only medium and no fluorescent-labeled compound. The different dilutions of pPB-HSA do cause an increase in MFI where the lowest dilution causes the highest MFI meaning that there is high binding to the PDGFβ-receptor in these cells which is concentration dependent. The higher the concentration of pPB-HSA, the higher the binding to the 3T3 cells can be seen. Because the 1µg/ml concentration of pPB-HSA still gives a high MFI response, this dilution has been used during the different experiments. This experiment shows that the peptide does bind to the cells and that it can be determined by using the cytoflex.

Binding of pPB-HSA and HSA to NIH3T3 fibroblasts

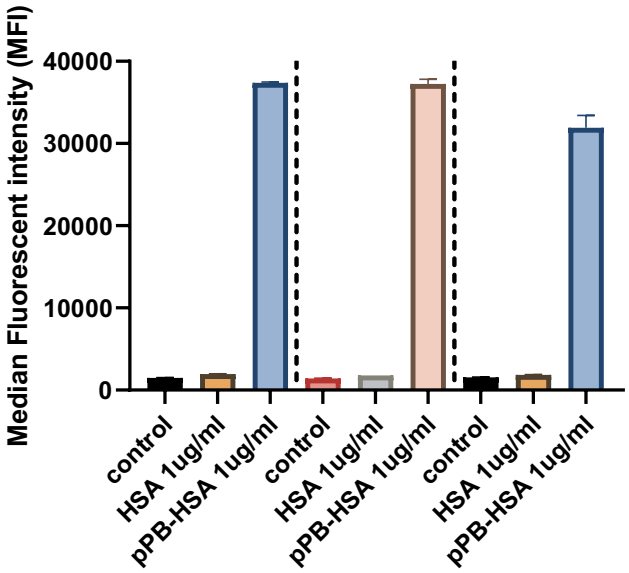

Graph 3: The binding of HSA and pPB-HSA to the 3T3 fibroblasts in vitro. The binding was measured using the cytoflex at 638 nm and the mean fluorescence intensity (MFI) of the binding of HSA and pPB-HSA was calculated. HSA was added in a concentration of 1ug/ml as well as pPB-HSA.

The last experiment showed that pPB-HSA binds to the 3T3 cells and is concentration dependent. Since pPB is coupled to HSA, the binding of both proteins to cells was compared to each other to test whether the binding of pPB-HSA is different from HSA itself. 50,000 3T3 cells were incubated for 24 hours after which pPB and HSA alone in a concentration of 1µg/ml was added to the cells. After an hour of incubation, the binding was measured by the cytoflex. The experiment was done in triplo and performed three times. All three of the experiments are shown in graph 3. Each dotted line in the graph separates the different experiments from each other.

Graph 3 shows the binding of HSA and pPB-HSA to the 3T3 fibroblasts. Three samples were measured. The first sample is the control which contained only medium. It can be seen that the MFI of the control is significantly lower than the cells that contained pPB-HSA. The MFI of HSA is similar to the MFI of the control indicating no binding of HSA to the 3T3 fibroblasts. The drastic increase of the pPB-HSA indicates a strong binding to these cells. This means that the peptide pPB is crucial for the binding of pPB-HSA to the cells.

Specificity of the binding of pPB-HSA to the PDGFß-receptor in NIH3T3 fibroblasts using PDGF-BB

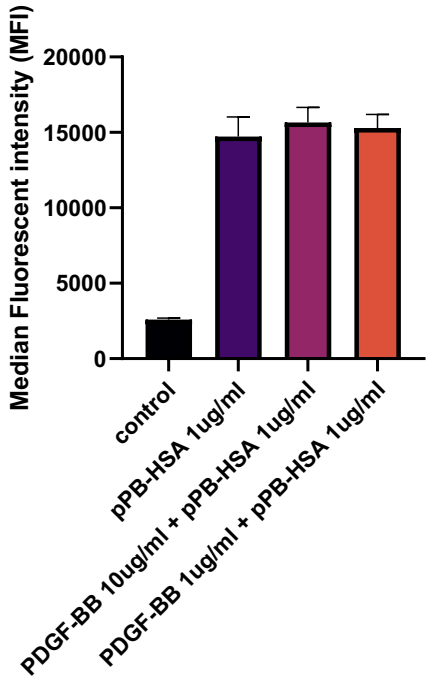

Graph 4: The binding of PDGF-BB and pPB-HSA to the 3T3 fibroblasts in vitro. The binding was measured using the cytoflex at a wavelength of 638 nm, and the mean fluorescence intensity (MFI) of $Alexa_{647}$ was calculated.

To determine the specificity of the binding of pPB-HSA to the 3T3 cells, PDGF-BB was added to act as a competitive inhibitor for the PDGFβ-receptor. In this experiment, 50,000 3T3 cells were plated in a 24-wells plate and incubated for 24 hours. pPB-HSA was added in a concentration of 1μg/ml after PDGF-BB was incubated for an hour in two different concentrations: 10μg/ml and 1μg/ml. pPB-HSA was added in the wells without removing the medium containing PDGF-BB. The binding was then measured with the cytoflex and the MFI was calculated.

Graph 4 shows the binding of pPB-HSA and the effect of PDGF-BB on the binding of pPB-HSA to the 3T3 fibroblasts. To the cells medium alone was added (control), 1μg/ml pPB-HSA and pre-incubation of PDGF-BB (10μg/ml and 1μg/ml) together with pPB-HSA. The control has a low MFI in comparison with the other three samples. pPB-HSA gives a rise in MFI but there is no significant difference between the addition of PDGF-BB and pPB-HSA alone. This applies to both concentrations of PDGF-BB. Pre-incubating PDGF-BB causes no effect in the binding of pPB-HSA to the 3T3 cells indicating no competition on the PDGFβ-receptor.

Specificity of the binding of pPB-HSA to the PDGFß-receptor in NIH3T3 fibroblasts using TGF-β

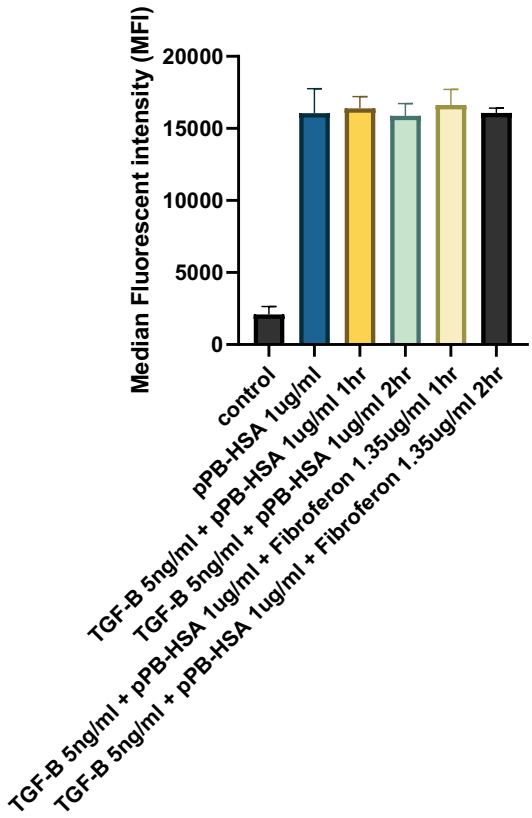

Graph 5: The effect of TGF-β (1h and 2h) and Fibroferon on the binding of pPB-HSA on the 3T3 fibroblasts. The binding was measured using the cytoflex at a wavelength of 638nm, and the mean fluorescence intensity (MFI) of Alexa$_{647}$ was calculated.

In the last experiment, PDGF-BB was used to determine the specificity of pPB-HSA which was shown in graph 4. Since no significant effect was seen, TGF-β was added since it activates the 3T3 cells and induced the production of PDGF-BB to achieve a competitive effect on the PDGFβ-receptor[10,29]. Since Fibroferon also binds to the PDGFβ-receptor, it was added as well for competition. In this experiment, 50,000 3T3 cells were plated in a 24-wells plate and incubated for 24 hours. Medium alone or TGF-β (5ng/ml) was then added one hour and two hours prior to the addition of pPB-HSA (1µg/ml) or pPB-HSA and Fibroferon (1.35µg/ml) together. After adding pPB-HSA or a mixture of pPB-HSA and Fibroferon, the cells were incubated again for an hour. The binding was then analyzed by the cytoflex. The experiment was done in triplo and performed twice of which the mean was calculated.

Graph 5 shows the mean of two experiments that studied the effect of TGF-β on the binding of pPB-HSA in 3T3 cells. The control shows no binding since the MFI is low. The MFI of the other samples show no significant difference between each other. There is an increase of MFI in comparison with the control but no difference between the other samples after addition of TGF-β or Fibroferon. Adding TGF-β to induce the production of PDGF-BB, as well as adding Fibroferon, showed no effect on the binding of pPB-HSA to the 3T3 cells indicating no competition on the PDGFβ-receptor.

Effect of compounds on the PDGFβ-receptor expression

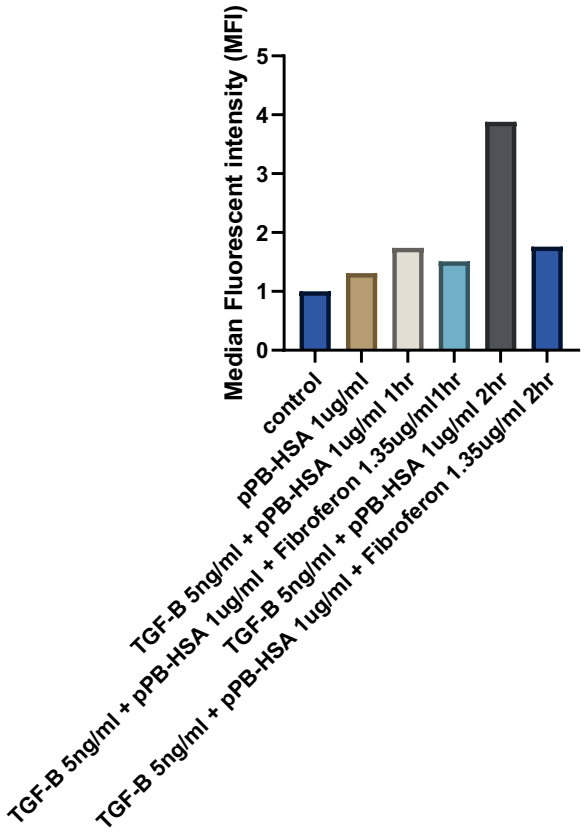

Graph 6: Effect of TGF-β (5ng/ml), pPB-HSA (1µg/ml) and Fibroferon (1.35µg/ml) on the PDGFβ-receptor mRNA expression in NIH3T3 fibroblasts. The expression levels were normalized by using β-actin as a household gene.

In the last experiment the effect of TGF-β on the binding of pPB-HSA to the 3T3 cells was investigated. To know whether the expression of the PDGFβ-receptor could play a role, a real-time PCR was performed to study the effects of the compounds on the receptor expression. The same compounds in the same concentrations as the previous experiment were added, and the gene expression was determined. The experiment was performed only once and not in triplo due to technical errors (N=1, n=1).

Graph 6 shows the quantitative real-time PCR analysis of PDGFβ-receptor in 3T3 cells that have been treated with pPB-HSA (1µg/ml) and TGF-β (5ng/ml) with pPB-HSA and Fibroferon (1.35µg/ml). The expression levels were normalized with β-actin. When the cells were treated with TGF-β and incubated for 2 hours after which pPB-HSA was added, the fold induction was the highest as is seen in graph 6. This indicates a higher expression of the PDGFβ-receptor. The control has the lowest fold induction whereas the other treatments gave a similar fold induction and thus expression of the receptor. This experiment shows that after a two hour incubation of TGF-β, the PDGFβ-receptor expression is induced.

Intracellular uptake of pPB-HSA in NIH3T3 fibroblasts

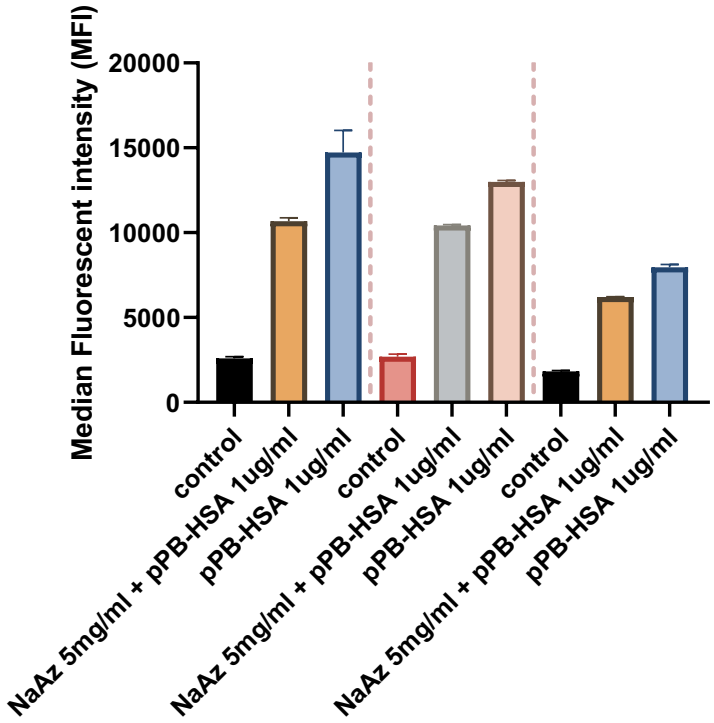

Graph 7: The effect of sodiumazide (NaAz) on the binding of pPB-HSA to the 3T3 fibroblasts in vitro. The binding was measured using the cytoflex at a wavelength of 638 nm, and the mean fluorescence intensity (MFI) of Alexa$_{647}$ was calculated.

In the previous experiments, the binding of pPB-HSA has been determined including the fact that pPB contributes to the binding since HSA alone does not bind. This experiment will look at the intracellular uptake of pPB-HSA. To determine this, sodium azide (NaAz) has been added which is an inhibitor of energy-dependent uptake processes[31-33]. In this experiment, 50,000 3T3 cells were plated in a 24-wells plate and incubated overnight. Medium alone (control) and pPB-HSA (1μg/ml) were added after the cells were incubated with or without sodium azide (5mg/ml) for an hour. The binding was then measured by the cytoflex. The experiment was done in triplo and performed three times.

Graph 7 shows the effect of sodium azide (NaAz) on the binding of pPB-HSA. Since the experiment was performed three times, all three of the results are shown in graph 7. The dotted line separates the three different experiments from each other. There can be seen that the addition of NaAz causes a reduction in the MFI in comparison with only pPB-HSA. All three of the experiments show a similar decrease of MFI after the addition of NaAz, although the overall fluorescence in the third experiment was somewhat lower. This experiment shows that NaAz inhibits a part of the binding of pPB-HSA (about 20%) to the 3T3 cells.

NO and MTT assay in 264.7 RAW macrophages

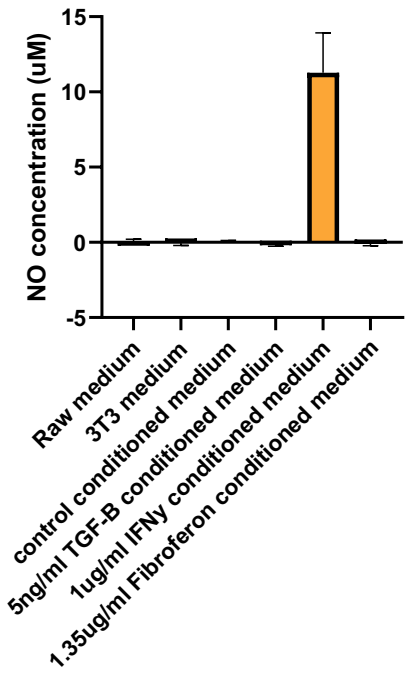

Graph 8: The NO assay in 264.7 RAW macrophages with different treatments. Conditioned medium of 3T3 cells with different treatments (medium alone, 5ng/ml TGF-β, 1µg/ml IFNγ and 1.35µg/ml Fibroferon) was added to the RAW cells. The NO was measured using a plate reader at 550nm.

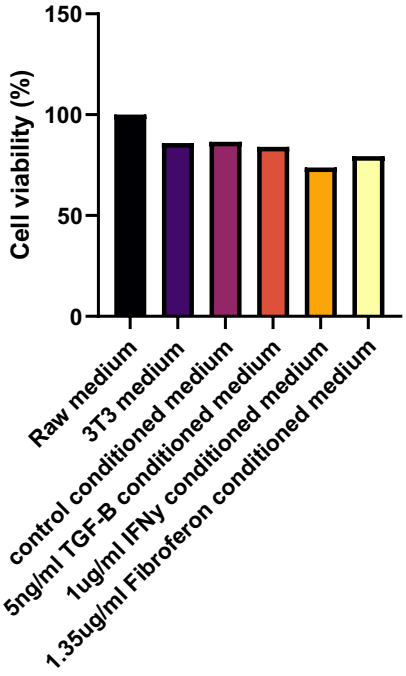

Graph 9: The MTT assay of 264.7 RAW macrophages showing the cell viability (%) of the macrophages after treatment with RAW medium, 3T3 medium and conditioned medium of the 3T3 cells containing different treatments (medium alone, 5ng/ml TGF-β, 1µg/ml IFNγ and 1.35µg/ml Fibroferon (n=1). The viability of the cells was measured using a plate reader at 550nm.

To analyze the anti-fibrotic effects of Fibroferon and IFNγ, RAW 264.7 cells were used in this experiment. Conditioned medium of 3T3 cells with different treatments were added to the RAW 264.7 cells to measure the effect of each treatment on the production of NO. Firstly, 50,000 3T3 cells were plated in a 24-wells plate and incubated overnight. Different treatments were then added (medium alone, 5ng/ml TGF-β, 1µg/ml IFNγ and 1.35µg/ml Fibroferon) and incubated for 24 hours. The conditioned medium was then added to the RAW cells and incubated for 24 hours after 100,000 cells in a 96-wells plate were incubated overnight. An NO assay was performed to measure the secreted nitrite. Subsequently, an MTT assay was also performed to measure the viability of the cells.

Graph 8 shows the NO assay that is performed in cultures of RAW macrophages. It can be seen that only IFNγ gave a NO concentration of around 11µM. The other treatments had no effect on the NO production of the cells. Graph 9 shows the cell viability of the macrophages. RAW medium alone gave the highest cell viability of 100%. The lowest cell viability was after the addition of conditioned medium that contained IFNγ followed by Fibroferon. Overall, the viability of the cells in all the treatments are around the same percentage. Graphs 8 and 9 show that Fibroferon binds specifically to the PDGFβ-receptor since no NO response was seen in contrast with IFNγ.

Anti-fibrotic effects of IFNγ and Fibroferon in NIH3T3 fibroblasts

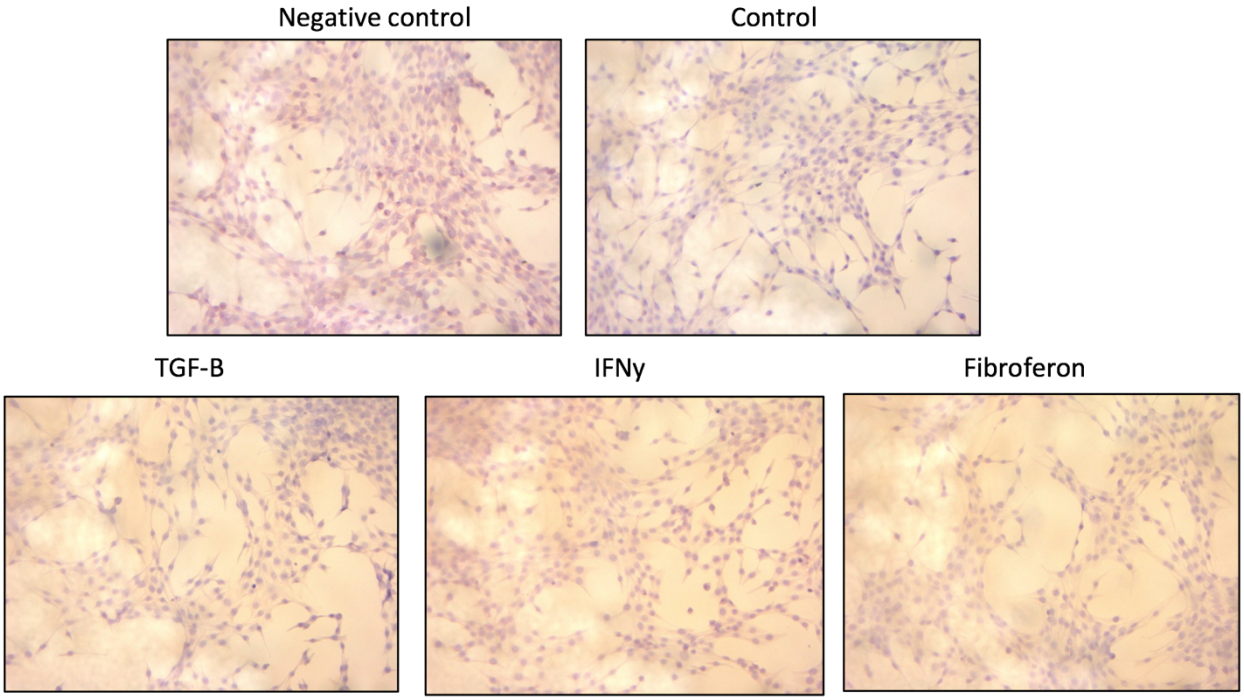

Figure 3: Immunohistochemical staining of α-SMA on 3T3 cells. The cells (50,000/well in a 24-wells plate) have been incubated for 24 hours after which the cells were activated by adding 5ng/ml TGF-β. After 24 hours the cells were treated with medium alone, 1μg/ml IFNγ and 1.35μg/ml Fibroferon and the cells were incubated again for 24 hours before performing the staining on α-SMA. The negative control contains no α-SMA antibody.

In the last experiment, the anti-fibrotic effects of IFNγ and Fibroferon were analyzed by using the RAW cells. In this experiment, the anti-fibrotic effects will be analyzed by performing an immunohistochemical staining of α-SMA since α-SMA is upregulated in fibrosis. Firstly, 50,000 cells were plated in a 24-wells plate and incubated overnight. To activate the cells, 5ng/ml TGF-β was added and incubated for another 24 hours. The cells were then treated with medium alone, 1μg/ml IFNγ and 1.35μg/ml Fibroferon. Figure 3 shows the immunohistochemical staining of α-SMA on 3T3 cells. All the different treatments show no sign of redness meaning that there is no α-SMA expression seen in these cells. Since no treatment showed any expression, no change can be observed between the different treatments of the cells. The anti-fibrotic effects could not be determined by performing the α-SMA staining.

Effect of TGF-β, IFNγ and Fibroferon on the intracellular collagen I in NIH3T3 fibroblasts

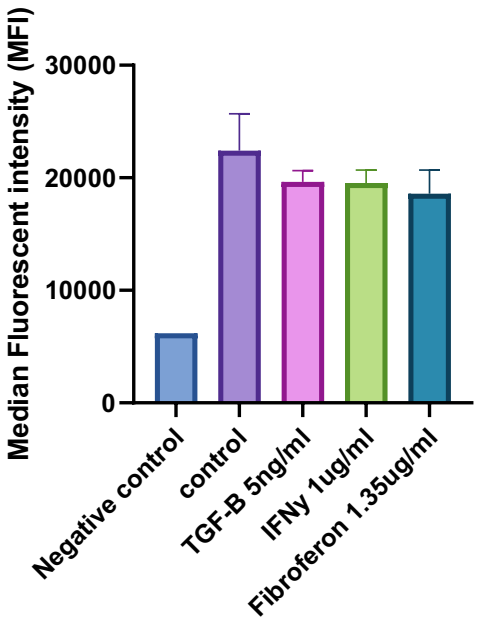

Graph 10: The FACS measurement of intracellular collagen I in 3T3 cells after the cells have been treated with 5ng/ml TGF-β, 1µg/ml IFNγ and 1.35µg/ml Fibroferon for 24 hours. The binding was measured by the cytoflex at a wavelength of 638 nm.

To again study the anti-fibrotic effects of IFNγ and Fibroferon on TGF-β induced 3T3 cells, a cytoflex measurement of intracellular collagen type I using the cytoflex has been done. Intracellular collagen I was measured since collagen is a marker for fibrosis and is mostly present intracellularly. The cells were incubated with 5ng/ml of TGF-ß for 24 hours to activate the cells after which the cells were treated with medium alone, 1µg/ml IFNγ and 1.35µg/ml Fibroferon. Collagen type I-antibody was added, and the cells were analyzed using the cytoflex at a wavelength of 638 nm. Graph 10 shows the MFI of the different treatments. There is no significant difference between the different treatments as they all have about the same MFI indicating the same amount of collagen I in the samples. The negative control shows a low MFI signal since the first antibody was not added in this sample. All the samples were performed in triplo except for the negative control. All the treatments showed a similar MFI signal indicating the same collagen I expression in every treatment.

5. Discussion

The aim of the thesis is to use the PDGFB-receptor as a target for anti-fibrotic therapies using pPB-HSA which specifically targets this receptor. The binding of pPB-HSA to the PDGF-BB receptor was studied as well as the specificity of the pPB-HSA to the PDGFB-receptor. Finally, the anti-fibrotic effects of IFNy and Fibroferon were also examined.

The binding of pPB-HSA was firstly examined by adding pPB-HSA in different concentrations (1µg/ml, 2µg/ml, 10µg/ml, and 20µg/ml). Graph 1 and graph 2 show different fluorescence intensities which indicates the amount of pPB-HSA that has been bound to the cells. The binding of pPB-HSA to cells was strongly correlated with the concentration. It showed a linear correlation. Since pPB-HSA is the only compound that is fluorescent, which is added to the cells, the fluorescent signal comes only from the binding of the peptide to the cells. This was also tested by adding only free dye of $Alexa_{647}$. This gave no increase in fluorescent intensity indicating no binding of the dye to the cells. The fluorescent labeling does not affect the binding of the peptide. Human serum albumin (HSA) was also added in the same concentration as pPB-HSA (1µg/ml) to see whether pPB contributes to the binding of the peptide to the cells or whether HSA also plays a role in this. HSA was coupled to $Alexa_{647}$ as well to get a fluorescent signal and measure the binding. Graph 3 shows the binding of HSA and pPB-HSA to the 3T3 fibroblasts. The fluorescence intensity of HSA is almost the same as the control whereas pPB-HSA shows a great increase of median fluorescence intensity (MFI). This shows that HSA alone does not bind the cells at all, and that pPB contributes to the binding to the PDGFß-receptor[10,15].

The specificity of this peptide was then examined by adding PDGF-BB. By adding PDGF-BB prior to the addition of pPB-HSA, competition is anticipated since both proteins have affinity for the same receptor. A decrease of binding of pPB-HSA is expected to be seen since the receptor is blocked by PDGF-BB. Two different concentrations were compared with each other (10µg/ml and 1µg/ml). After an hour, 1µg/ml pPB-HSA was added. As is seen in graph 4, there is no significant difference between the addition of PDGF-BB and pPB-HSA alone. There was also no significant difference seen between the two concentrations of PDGF-BB. Since both PDGF-BB and pPB-HSA have affinity for the same receptor, there was expected to see a reduction in binding of pPB-HSA to the cells since the receptor is already blocked by PDGF-BB. The fact that there is no difference seen in the MFI after the pre-incubation with PDGF-BB can be due to the fact that either pPB-HSA does not bind the PDGFß-receptor or that pPB-HSA has a higher affinity to the receptor than PDGF-BB does. Another factor that could play a role is the incubation time. PDGF-BB was added an hour before the addition of pPB-HSA to be sure that PDGF-BB would bind to the receptor before pPB-HSA does. Since no effect was seen, it could be that PDGF-BB has already been taken up by the cells causing no competitive effect. In the previous experiment, it has been concluded that pPB contributes to the binding of the 3T3 cells and HSA alone does not bind. Therefore, it is not likely that pPB-HSA does not bind the PDGFß-receptor and thus have no competitive effect with PDGF-BB. The fact that no significant difference is seen between the two samples can be due to a wrong incubation time. To achieve a competitive effect, both peptides can be added together at the same time to the cells to see whether there is decrease in binding of pPB-HSA indicating specificity to the PDGFß-receptor.

The specificity was also determined by adding TGF-ß instead of PDGF-BB. When TGF-ß is added to the cells, it can promote the cells into producing PDGF-BB[26,31,34]. This can then bind to the PDGFß-receptor and cause blocking of the binding of pPB-HSA to the same receptor. This way, the specificity can be determined. The binding of pPB-HSA to the receptor is expected to be decreased which will also lead to a lower MFI. TGF-ß (5ng/ml) was added an hour and two hours before adding pPB-HSA. The experiment was repeated two times. Graph 5 shows the mean of two experiments that were performed. The control shows a low MFI signal since no fluorescent-labeled compound was added. The rest of the treatments show no decrease of MFI (and thus binding of pPB-HSA to the 3T3 cells) when treated with TGF-ß or a combination of TGF-ß and Fibroferon. This can be explained by the fact that TGF-ß does not only increase the production of PDGF-BB but also increases the expression of the PDGFß-receptor, which can be seen in graph 6 where the PCR shows a high expression of the PDGFβ-receptor after two hour of incubation with TGF-β. This leads to more binding sites where PDGF-BB can bind as well as pPB-HSA and thus no competitive effect. Another explanation is the incubation time of TGF-ß. It is not clear what incubation time is needed for TGF-ß to produce a right amount of PDGF-BB. It can be that more time is needed to produce PDGF-BB and to witness a competitive effect. Because of lack of time this was not examined and can be done in the future.

To know whether the expression of the PDGFß-receptor is increased, a PCR has been done to examine the expression of the receptor. Graph 8 shows the fold induction of the PDGFß-receptor. There can be seen that the different samples cause around the same expression of the receptor except for the treatment with TGF-ß which was incubated for 2 hours after which pPB-HSA was added. There is a strong increase in expression of the PDGFß-receptor. Even though the expression of the receptor is increased, there was no increase in binding of pPB-HSA since the MFI is not increased in graph 5. This can be explained by the fact that TGF-ß causes an increase in receptor expression but also an increase in the production of PDGF-BB[28,29,30]. PDGF-BB also has affinity for the PDGFß-receptor as well as pPB-HSA leading to no increase in binding of pPB-HSA to the receptor since PDGF-BB has been already bound. The experiment was performed once meaning that the results are not accurate. Repeating the experiment 2 more times can increase the reliability of the results and reduce the effect of errors. To know whether PDGF-BB is produced by TGF-ß as well, a PCR can be performed in the future to study the expression of PDGF-BB. Induction of the expression of PDGF-BB can confirm the hypothesis that the PDGF-BB production is induced as well as the expression of the PDGFß-receptor leading to no decrease in binding of pPB-HSA in 3T3 cells.

The intracellular uptake of pPB-HSA has also been examined by adding sodium azide (5mg/ml) an hour prior to the addition of pPB-HSA. Sodium azide inhibits oxidative phosphorylation via inhibition of cytochrome oxidase, the final enzyme in the mitochondrial electron transport chain, thereby resulting in a rapid depletion of intracellular ATP[32,33,35]. Graph 7 shows the effect of sodium azide on the uptake of pPB-HSA in 3T3 cells. The experiment has been performed in triplo and repeated three times. The control shows a low MFI since no fluorescent labeled compound has been added. pPB-HSA has a high increase of binding since the MFI is also high. Sodium azide reduces the MFI meaning that less pPB-HSA is bound to the cells. The MFI is still significantly higher than the control meaning that there is energy-dependent and energy-independent binding and uptake. The binding is probably energy-independent (80% of the MFI) whereas the uptake is probably energy-dependent (20% of the

MFI). Internalization of pPB-HSA is energy consuming and thus needs energy which is inhibited by sodium azide. The amount of binding of pPB-HSA that is reduced is the amount of pPB-HSA that is taken up into the cell since the binding has been decreased after inhibition of energy. There is still a signal of binding of pPB-HSA to the cells which is either not taken up intracellularly or it is taken up passively, without consuming energy. This does show that a part of pPB-HSA is internalized which gives a good perspective for modification of the peptide for future experiments.

After investigating the binding of pPB-HSA to the 3T3 cells, the antifibrotic effects of Interferon gamma (IFNγ) and Fibroferon were investigated. Fibroferon is known to have less adverse effects then IFNγ since it specifically binds to the PDGFß-receptor in contrast with IFNγ. IFNγ is known to have more adverse effects due to more expression of the IFNγ-receptor in the body[10,30]. To measure the adverse effects, an NO assay was done by using the 264.7 RAW macrophages. The cells were treated with TGF-ß to induce fibrosis after which fibrosis was reduced by adding IFNγ and Fibroferon since they both have antifibrotic effects[10,26,29]. The conditioned medium of the 3T3 cells were then added to the RAW cells to look at the effect on the macrophages. NO is produced by these cells when there is damage or inflammation and especially when there is IFNγ. Adding IFNγ to the 3T3 cells will lead to a high NO production since IFNγ causes an M1 configuration[10,29]. Fibroferon is IFNγ that is bound to a peptide which is specific for the PDGFß-receptor[10]. Expected is that the cells treated with Fibroferon will lead to a lower NO production since most of the Fibroferon will be bound to the 3T3 cells, due to its specificity for the PDGFß-receptor, leading to less Fibroferon in the conditioned medium. Graph 8 shows the NO assay of the different treatments. RAW medium and 3T3 medium was also added separately to see whether the medium alone would affect the production of NO in macrophages. The graph shows for all the treatments no NO production except for the treatment with IFNγ. This is in line with the expectation that IFNγ would lead to an induction of NO production and Fibroferon a decrease in comparison with IFNγ. That Fibroferon lead to no NO production in the RAW cells is either because the peptide is not functional or all of it is bound to the 3T3 cells leaving no Fibroferon in the conditioned medium. This would mean that Fibroferon binds more specific to the 3T3 cells than IFNγ, leading to less NO production in the macrophages. This is in line with the fact that Fibroferon has less IFNγ-related side effects in vivo since the 264.7 RAW macrophages do not express the PDGFß-receptor but do express the IFNγ-receptor[10].

An MTT assay was also done to measure the cell viability of the cells. The viability is measured as a percentage of the control which can be seen in graph 9. It was expected that all the treatments would lead to a minimal decrease in cell viability since the treatments do not cause the production of NO or do not cause harm to the cells, except for IFNγ. IFNγ is a pro-inflammatory cytokine but works antifibrotic. It can polarize the macrophages into the M1 configuration and cause production of NO. Because it is a pro-inflammatory cytokine, it can decrease the cell viability[10,29]. This is also seen in graph 9. Only IFNγ shows a clear decrease in comparison with the other treatments which is in line with the expectation. Since the other treatments had a quite high cell viability, it can be concluded that the reason that no NO is produced is not caused by damage or dying of the cells but it is because the treatment led to no NO production in the macrophages.

Another experiment to examine the antifibrotic effects of IFNγ and Fibroferon was done by performing an immunohistochemical staining of a-smooth muscle actin (α-SMA) on 3T3 cells. α-SMA is a marker for fibrosis which is used to detect the effect of different treatments on myofibroblasts[4,5]. In this experiment, the cells were activated by adding TGF-ß (5ng/ml) after which IFNγ (1µg/ml) was added and Fibroferon (1.35µg/ml) to see whether cell activation can be reduced since both IFNγ and Fibroferon have antifibrotic effects. Figure 3 shows the staining of the 3T3 cells with the different treatments. There was also a negative control where no α-SMA antibody was added. As seen in figure 3, no staining of α-SMA is seen in all the treatments since no red color can be observed. It is unlikely that no α-SMA is in the different treatments, especially after the addition of TGF-ß, since α-SMA is usually present in the cell without the induction of fibrosis[4,5]. The reason that the immunohistochemical staining did not show any α-SMA can be due to a technical error. The experiment needs to be repeated in the future.

The last experiment that was done is to check the effect of IFNγ and Fibroferon on the production of collagen I in 3T3 cells after fibrosis has been induced. This way, the antifibrotic effects of both peptides can be examined. Because TGF-ß induces fibrosis, the MFI of this treatment should be induced since collagen I is a marker for fibrosis[4,5,1]. After the addition of IFNγ and Fibroferon, the MFI is expected to be decreased since they both have antifibrotic effects. Because Fibroferon binds more specific to the 3T3 cells, the collagen I is expected to be lower than when IFNγ is added. The collagen I expression is measured for the first time by using the cytoflex. The results can be seen in graph 12. There is no significant difference between the different measurements. The control shows the highest MFI meaning the highest collagen I expression which is not in line with the hypothesis since TGF-ß induces fibrosis and the collagen I expression is thus expected to be the highest with this treatment. There were also no significant differences between the cells treated with TGF-ß, IFNγ or Fibroferon compared to untreated cells. A negative control was tested, that is, incubations where the anti-collagen I antibody was omitted. In graph 10 it can be seen that the negative control shows a low MFI indicating that the signal is induced by the collagen I antibody. There was only one sample of negative control which is why no standard deviation could be calculated. Since there is no significant difference between the different treatments, there can be concluded that IFNγ and Fibroferon had no effect on the collagen I expression. On the other hand, there was an MFI signal seen meaning that the cytoflex can be used in future experiments to measure the collagen I expression in the 3T3 cells.

Conclusion

The aim of the thesis was to examine whether the PDGFß-receptor can be used as a target for antifibrotic therapies by application of the PDGF-receptor binding peptide pPB. Since pPB-HSA caused a high increase in binding to the 3T3 cells and HSA showed no binding, it can be concluded that pPB contributes to the binding and is needed to bind to the 3T3 cells. The specificity of pPB-HSA could not be determined by using PDGF-BB as a competitive inhibitor. The incubation time of PDGF-BB can be changed in the future by adding pPB-HSA and PDGF-BB at the same time which can lead to better results. Another way to determine the specificity is by adding a PDGFß-receptor antibody to block the receptor and see whether the binding of pPB-HSA would decrease or that no change would be seen. The results also showed a significant difference when sodium azide was added in comparison with only pPB-HSA which indicated that pPB-HSA is partly taken up intracellularly via an active way since sodium azide inhibits the energy intracellularly. This gives a great perspective of the uptake of the peptide intracellularly but also for future experiments to look into the uptake of pPB-HSA in the nucleus. The antifibrotic effects of IFNγ and Fibroferon were determined by an NO and MTT assay which showed no NO response when Fibroferon was used in contrast to IFNγ which was as expected since most of the Fibroferon was probably bound to the 3T3 cells due to its specificity for the PDGFß-receptor. The effects of IFNγ and Fibroferon on α-SMA production in the fibroblasts could not be determined since the staining was not performed correctly. This can be repeated in the future to see whether the antifibrotic effects of IFNγ and Fibroferon can be studied by an α-SMA staining. Instead of using α-SMA as a fibrotic marker, collagen I was used and determined by using the cytoflex. It was concluded that IFNγ and Fibroferon had no effect on the collagen I expression in 3T3 cells. This thesis shows that the binding of pPB-HSA to the 3T3 cells can be determined by using the cytoflex and that the peptide pPB contributes to the binding. The PDGFß-receptor was used as a target for antifibrotic therapies which showed promising effects for future experiments.

References

1. Bansal, R. (2012). Re-direction of interferon gamma and its signaling moiety : new options for the therapy of chronic deseases. [S.l. : s.n.], cop. 2012.
2. Weng, H. L., Wang, B. E., Jia, J. D., Wu, W. F., Xian, J. Z., Mertens, P. R., Cai, W. M., & Dooley, S. (2005). Effect of Interferon-Gamma on Hepatic Fibrosis in Chronic Hepatitis B Virus Infection: A Randomized Controlled Study. *Clinical Gastroenterology and Hepatology*, *3*(8), 819–828. https://doi.org/10.1016/s1542-3565(05)00404-0
3. Bataller, R., & Brenner, D. A. (2005). Liver fibrosis. *Journal of Clinical Investigation*, *115*(2), 209–218. https://doi.org/10.1172/jci24282
4. Iwaisako, K., Brenner, D. A., & Kisseleva, T. (2012). What's new in liver fibrosis? The origin of myofibroblasts in liver fibrosis. *Journal of Gastroenterology and Hepatology*, *27*, 65–68. https://doi.org/10.1111/j.1440-1746.2011.07002.x
5. Acharya, P., Chouhan, K., Weiskirchen, S., & Weiskirchen, R. (2021b). Cellular Mechanisms of Liver Fibrosis. *Frontiers in Pharmacology*, *12*. https://doi.org/10.3389/fphar.2021.671640
6. Ying, H. Z., Chen, Q., Zhang, W. Y., Zhang, H. H., Ma, Y., Zhang, S. Z., Fang, J., & Yu, C. H. (2017). PDGF signaling pathway in hepatic fibrosis pathogenesis and therapeutics. *Molecular Medicine Reports*, *16*(6), 7879–7889. https://doi.org/10.3892/mmr.2017.7641
7. Roehlen, N., Crouchet, E., & Baumert, T. F. (2020). Liver Fibrosis: Mechanistic Concepts and Therapeutic Perspectives. *Cells*, *9*(4), 875. https://doi.org/10.3390/cells9040875
8. McQuitty, C. E., Williams, R., Chokshi, S., & Urbani, L. (2020). Immunomodulatory Role of the Extracellular Matrix Within the Liver Disease Microenvironment. *Frontiers in Immunology*, *11*. https://doi.org/10.3389/fimmu.2020.574276
9. Duarte, S., Baber, J., Fujii, T., & Coito, A. J. (2015b). Matrix metalloproteinases in liver injury, repair and fibrosis. *Matrix Biology*, *44–46*, 147–156. https://doi.org/10.1016/j.matbio.2015.01.004
10. Van Dijk, F., Olinga, P., Poelstra, K., & Beljaars, L. (2015). Targeted Therapies in Liver Fibrosis: Combining the Best Parts of Platelet-Derived Growth Factor BB and Interferon Gamma. *Frontiers in Medicine*, *2*. https://doi.org/10.3389/fmed.2015.00072
11. Chen, P. H., Chen, X., & He, X. (2013). Platelet-derived growth factors and their receptors: Structural and functional perspectives. *Biochimica et Biophysica Acta (BBA) - Proteins and Proteomics*, *1834*(10), 2176–2186. https://doi.org/10.1016/j.bbapap.2012.10.015
12. Bera, A., Das, F., Ghosh-Choudhury, N., Li, X., Pal, S., Gorin, Y., Kasinath, B. S., Abboud, H. E., & Ghosh Choudhury, G. (2014). A positive feedback loop involving Erk5 and Akt turns on mesangial cell proliferation in response to PDGF. *American Journal of Physiology-Cell Physiology*, *306*(11), C1089–C1100. https://doi.org/10.1152/ajpcell.00387.2013
13. Bonner, J. C. (2004). Regulation of PDGF and its receptors in fibrotic diseases. *Cytokine & Growth Factor Reviews*, *15*(4), 255–273. https://doi.org/10.1016/j.cytogfr.2004.03.006
14. Tsioumpekou, M., Cunha, S. I., Ma, H., Åhgren, A., Cedervall, J., Olsson, A. K., Heldin, C. H., & Lennartsson, J. (2020). Specific targeting of PDGFRβ in the stroma inhibits

growth and angiogenesis in tumors with high PDGF-BB expression. *Theranostics*, *10*(3), 1122–1135. https://doi.org/10.7150/thno.37851
15. Beljaars, L., Weert, B., Geerts, A., Meijer, D. K., & Poelstra, K. (2003). The preferential homing of a platelet derived growth factor receptor-recognizing macromolecule to fibroblast-like cells in fibrotic tissue. *Biochemical Pharmacology*, *66*(7), 1307–1317. https://doi.org/10.1016/s0006-2952(03)00445-3
16. Heldin, C. H. (2012). Autocrine PDGF stimulation in malignancies. *Upsala Journal of Medical Sciences*, *117*(2), 83–91. https://doi.org/10.3109/03009734.2012.658119
17. Teekamp, N., Van Dijk, F., Broesder, A., Evers, M., Zuidema, J., Steendam, R., Post, E., Hillebrands, J., Frijlink, H., Poelstra, K., Beljaars, L., Olinga, P., & Hinrichs, W. (2017). Polymeric microspheres for the sustained release of a protein-based drug carrier targeting the PDGFβ-receptor in the fibrotic kidney. *International Journal of Pharmaceutics*, *534*(1–2), 229–236. https://doi.org/10.1016/j.ijpharm.2017.09.072
18. Prakash, J., De Jong, E., Post, E., Gouw, A. S., Beljaars, L., & Poelstra, K. (2010). A novel approach to deliver anticancer drugs to key cell types in tumors using a PDGF receptor-binding cyclic peptide containing carrier. *Journal of Controlled Release*, *145*(2), 91–101. https://doi.org/10.1016/j.jconrel.2010.03.018
19. Jablonski, K. A., Amici, S. A., Webb, L. M., Ruiz-Rosado, J. D. D., Popovich, P. G., Partida-Sanchez, S., & Guerau-de-Arellano, M. (2015). Novel Markers to Delineate Murine M1 and M2 Macrophages. *PLOS ONE*, *10*(12), e0145342. https://doi.org/10.1371/journal.pone.0145342
20. Yunna, C., Mengru, H., Lei, W., & Weidong, C. (2020). Macrophage M1/M2 polarization. *European Journal of Pharmacology*, *877*, 173090. https://doi.org/10.1016/j.ejphar.2020.173090
21. Redirecting Interleukin-10 in the Fibrotic liver: Effects on the Pathogenesis – Adriana Mattos
22. Italiani, P., & Boraschi, D. (2014). From Monocytes to M1/M2 Macrophages: Phenotypical vs. Functional Differentiation. *Frontiers in Immunology*, *5*. https://doi.org/10.3389/fimmu.2014.00514
23. Chi, D. S., Qui, M., Krishnaswamy, G., Li, C., & Stone, W. (2003). Regulation of nitric oxide production from macrophages by lipopolysaccharide and catecholamines. *Nitric Oxide*, *8*(2), 127–132. https://doi.org/10.1016/s1089-8603(02)00148-9
24. Fang, F. C., & Vazquez-Torres, A. (2002). Nitric oxide production by human macrophages: there's NO doubt about it. *American Journal of Physiology-Lung Cellular and Molecular Physiology*, *282*(5), L941–L943. https://doi.org/10.1152/ajplung.00017.2002
25. Weng, H. L., Wang, B. E., Jia, J. D., Wu, W. F., Xian, J. Z., Mertens, P. R., Cai, W. M., & Dooley, S. (2005). Effect of Interferon-Gamma on Hepatic Fibrosis in Chronic Hepatitis B Virus Infection: A Randomized Controlled Study. *Clinical Gastroenterology and Hepatology*, *3*(8), 819–828. https://doi.org/10.1016/s1542-3565(05)00404-0
26. Castro, F., Cardoso, A. P., Gonçalves, R. M., Serre, K., & Oliveira, M. J. (2018). Interferon-Gamma at the Crossroads of Tumor Immune Surveillance or Evasion. *Frontiers in Immunology*, *9*. https://doi.org/10.3389/fimmu.2018.00847
27. Horras, C. J., Lamb, C. L., & Mitchell, K. A. (2011). Regulation of hepatocyte fate by interferon-γ. *Cytokine & Growth Factor Reviews*, *22*(1), 35–43. https://doi.org/10.1016/j.cytogfr.2011.01.001

28. Borden, E. C., Sen, G. C., Uze, G., Silverman, R. H., Ransohoff, R. M., Foster, G. R., & Stark, G. R. (2007). Interferons at age 50: past, current and future impact on biomedicine. *Nature Reviews Drug Discovery*, *6*(12), 975–990. https://doi.org/10.1038/nrd2422
29. Schroder, K., Hertzog, P. J., Ravasi, T., & Hume, D. A. (2003). Interferon-γ: an overview of signals, mechanisms and functions. *Journal of Leukocyte Biology*, *75*(2), 163–189. https://doi.org/10.1189/jlb.0603252
30. Poosti, F., Bansal, R., Yazdani, S., Prakash, J., Beljaars, L., Van den Born, J., De Borst, M. H., Van Goor, H., Hillebrands, J. L., & Poelstra, K. (2016). Interferon gamma peptidomimetic targeted to interstitial myofibroblasts attenuates renal fibrosis after unilateral ureteral obstruction in mice. *Oncotarget*, *7*(34), 54240–54252. https://doi.org/10.18632/oncotarget.11095
31. Harvey, J., Hardy, S. C., & Ashford, M. L. J. (1999). Dual actions of the metabolic inhibitor, sodium azide on K_{ATP}channel currents in the rat CRI-G1 insulinoma cell line. *British Journal of Pharmacology*, *126*(1), 51–60. https://doi.org/10.1038/sj.bjp.0702267
32. Okano, T., Yamada, N., Okuhara, M., Sakai, H., & Sakurai, Y. (1995). Mechanism of cell detachment from temperature-modulated, hydrophilic–hydrophobic polymer surfaces. *The Biomaterials: Silver Jubilee Compendium*, 109–115. https://doi.org/10.1016/b978-008045154-1.50015-0
33. Zuo, Y., Hu, J., Xu, X., Gao, X., Wang, Y., & Zhu, S. (2019). Sodium azide induces mitochondria-mediated apoptosis in PC12 cells through Pgc-1α-associated signaling pathway. *Molecular Medicine Reports*. https://doi.org/10.3892/mmr.2019.9853
34. Porsch, H., Mehić, M., Olofsson, B., Heldin, P., & Heldin, C. H. (2014). Platelet-derived Growth Factor β-Receptor, Transforming Growth Factor β Type I Receptor, and CD44 Protein Modulate Each Other's Signaling and Stability. *Journal of Biological Chemistry*, *289*(28), 19747–19757. https://doi.org/10.1074/jbc.m114.547273
35. Jablonski, K. A., Amici, S. A., Webb, L. M., Ruiz-Rosado, J. D. D., Popovich, P. G., Partida-Sanchez, S., & Guerau-de-Arellano, M. (2015). Novel Markers to Delineate Murine M1 and M2 Macrophages. *PLOS ONE*, *10*(12), e0145342. https://doi.org/10.1371/journal.pone.0145342
36. Aydin, M. M., & Akcali, K. C. (2018). Liver fibrosis. *The Turkish Journal of Gastroenterology*, *29*(1), 14–21. https://doi.org/10.5152/tjg.2018.17330
37. Dooley, S., Hamzavi, J., Breitkopf, K., Wiercinska, E., Said, H. M., Lorenzen, J., Ten Dijke, P., & Gressner, A. M. (2003). Smad7 prevents activation of hepatic stellate cells and liver fibrosis in rats. *Gastroenterology*, *125*(1), 178–191. https://doi.org/10.1016/s0016-5085(03)00666-8
38. Karin, D., Koyama, Y., Brenner, D., & Kisseleva, T. (2016). The characteristics of activated portal fibroblasts/myofibroblasts in liver fibrosis. *Differentiation*, *92*(3), 84–92. https://doi.org/10.1016/j.diff.2016.07.001
39. Dooley, S., Hamzavi, J., Breitkopf, K., Wiercinska, E., Said, H. M., Lorenzen, J., Ten Dijke, P., & Gressner, A. M. (2003). Smad7 prevents activation of hepatic stellate cells and liver fibrosis in rats. *Gastroenterology*, *125*(1), 178–191. https://doi.org/10.1016/s0016-5085(03)00666-8
40. Zhubanchaliyev, A., Temirbekuly, A., Kongrtay, K., Wanshura, L. C., & Kunz, J. (2016). Targeting Mechanotransduction at the Transcriptional Level: YAP and BRD4 Are Novel Therapeutic Targets for the Reversal of Liver Fibrosis. *Frontiers in Pharmacology*, *7*. https://doi.org/10.3389/fphar.2016.00462

41. Aoto, K., Ito, K., & Aoki, S. (2018). Complex formation between platelet-derived growth factor receptor β and transforming growth factor β receptor regulates the differentiation of mesenchymal stem cells into cancer-associated fibroblasts. *Oncotarget*, *9*(75), 34090–34102. https://doi.org/10.18632/oncotarget.26124
42. Borkham-Kamphorst, E., & Weiskirchen, R. (2016). The PDGF system and its antagonists in liver fibrosis. *Cytokine & Growth Factor Reviews*, *28*, 53–61. https://doi.org/10.1016/j.cytogfr.2015.10.002

Appendices

Appendix 1: Protocols

1.1 Synthesis of $Alexa_{647}$-coupled pPB-HSA and $Alexa_{647}$-coupled HSA

pPB-HSA was diluted with 0.1M sodium carbonate buffer (pH = 8.3) to achieve a concentration of 10mg/ml. $Alexa_{555}$ was dissolved in an acetonitril:methanol (1:1 ratio) to a concentration of 10mg/ml and was aliquoted into 5µl tubes after freeze-drying and removing the solvent. The $Alexa_{555}$ aliquot was dissolved in 5µl of dry DMSO. 2.5 µl of $Alexa_{647}$ was added to 10 µl of pPB-HSA with 87,5 µl of 0.1M sodium carbonate buffer. The tubes were incubated for 2h at room temperature, while continuous stirring on the vortex and covered with aluminum foil. Pall Nanosept 3k filters were used to dialyze the construct. For pre-treatment, the filters were washed with PBS twice. The labeled compound was then added with 400µl of PBS onto the column and spun at 8000 rcf 5 min. The wash was done for 5-6 times after which the labeled construct was transferred to a fresh low-binding tube. This was then aliquoted into 5µl aliquotes and stored at -20˚C.

1.2 Measuring binding of pPB-HSA and other compounds with the FACS

Cells (50.000 cells/well) were plated in a 24-wells culture plate and incubated for 24 hours. Subsequently, the medium was removed and medium alone and pPB-HSA was added. In case of an inhibitory effect, the "inhibitor" was added 1 hour prior to the addition of pPB-HSA where the medium was not removed but pPB-HSA was added on top of the treatment. The cells were incubated again for 1 hour after which the medium was removed, and the cells were washed with 1ml of medium and 500µl of PBS twice. Subsequently, 250µl of TEP was added and the plate was incubated for 5 minutes in the stove. Then, 500µl of medium was added, and the cells were transferred to FACS-tubes. The tubes were centrifuged for 5 min at 300 g and the supernatant was discarded. The cells were eventually resuspended with 100µl of PBS and measured with the cytoflex.

1.3 Immunocytochemical staining

3T3 cells (50.000 cells/well) were plated in a 24-well culture plate with sterile plastic cover slips and incubated for 24 hours at 37˚C with 5% CO_2. After 24 hours, medium alone and 5 ng/ml of human recombinant TGFß1 was added and incubated for another 24 hours. Then the cells were incubated with medium alone, 1µg/ml IFNγ and 1,35µg/ml Fibroferon for 24 hours. The cells were fixed using methanol:aceton (1:1 ratio), dried and stored at -20˚C. The immunocytochemical staining was done the day after by rehydrating the coverslips with PBS after 30 minutes of drying under the ventilator. It was then incubated with the monoclonal mouse anti-α-SMA (Sigma) antibody (diluted with PBS) for 1 hour on parafilm with the cover slips upside down. The cover slips were then washed three times with fresh PBS and incubated with the polyclonal rabbit anti-mouse (Southern Biotech) antibody (diluted with PBS+5% NMS) for 30 minutes. The cover slips were then washed again for three times with fresh PBS and incubated with the polyclonal goat anti-rabbit antibody for 30 minutes (diluted with PBS+5% NMS). The slips were washed three times with fresh PBS. After 30 minutes the cells were stained with the NovaRed staining kit as per manufacturer's instructions. The cover slips were washed with demi-water and counterstaining with hematoxylin was performed for 1 minute.

The slips were washed with tap-water and the cells were mounted with DEPEX. After this, the cells were visualized using a light microscope.

Table 1: Antibodies used for the immunocytochemistry in 3T3 cells including their source and the dilution that was used in the experiment.

Antibody	*Source*	*Dilution*
Monoclonal mouse anti-α-SMA	Sigma	1:1000
Polyclonal rabbit anti-mouse	Southern Biotech	1:100
Polyclonal goat anti-rabbit	Southern Biotech	1:100

1.4 Intracellular FACS-staining of collagen I in 3T3 fibroblasts

3T3 cells (50.000/well) were plated in a 24-well culture plate and incubated for 24 hours at 37˚C with 5% CO_2. After 24 hours, medium alone and 5 ng/ml of human recombinant TGFß1 was added and incubated for another 24 hours. Then the cells were incubated with medium alone, 1µg/ml IFN and 1.35µg/ml Fibroferon for 24 hours. Subsequently, the cells were washed with medium and twice with PBS after which they were incubated with TEP (487,5 ml PBS, 10 ml 2,5% trypsin and 2,5ml sterile EDTA) for 5 min to get them off the wells. Medium was added and the cells were transferred to FACS tubes and centrifuged for 5 min at 300 g at 4˚C. The supernatant was discarded, and the pellet was resuspended with Fix/Perm (eBioscience) and incubated for 30 minutes on ice (4˚C). The tubes were centrifuged at 300 g for 5 min at 4˚C and the supernatant was discarded again. The cells were then incubated with the primary antibody Goat anti-type I collagen I (Southern Biotech) for 1 hour on ice. After an hour, the cells were centrifuged and vortexed with Perm Buffer (eBioscience) and centrifuged again. The cell pellet was incubated with the second antibody Donkey anti-goat IgG-FITC (Biotechnology) for 30 minutes on ice. After incubation, the FACS tubes were centrifuged for 5 min and the supernatant was discarded. Perm Buffer (eBioscience) was added, and the cells were centrifuged twice for 5 min. The cell pellet was resuspended with PFE (PBS, 2% FBS and 5mM EDTA) after which the samples were measured with the use of the Flow Cytometry (European Research Council).

Table 2: Antibodies used for the intracellular FACS-staining of collagen I in 3T3 cells including their source and the dilution that was used in the experiment.

Antibody	*Source*	*Dilution*
Goat anti-type I collagen	Southern Biotech	1:200
Donkey anti-goat IgG-FITC	Biotechnology	1:200

1.5 Quantitative real-time PCR

Total RNA from 3T3 fibroblasts was isolated using the Maxwell simplyRNA kit (Promega) according to Manufacturer's instructions. The RNA concentration was measured on a Nanodrop spectrophotometer (Nanodrop Technologies). Total RNA (~50ng/µl) was reverse transcribed by using the cDNA synthesis kit (Promega) in a volume of 50µl. The primers that were used and the sequences can be found in appendix 1.6. For the quantitative real time PCR analysis, 20ng of cDNA was used. For performing the reactions, SYBR green PCR master mix (Applied Biosystems) was used and performed according to the manufacturer's instructions. The reactions were analyzed by using the detection system. The housekeeping gene b-actin was used to normalize the relative gene expression.

Table 3: Sequence (5'-3') of the primers used for quantitative real-time PCR.

Gene	*Forward*	*Reverse*
b-actin	ATCGTGCGTGACATCAAAGA	ATGCCACAGGATTCCATACC
PDGFR-B	AACCCCCTTACAGCTGTCCT	TTCCTCTCATTGCCCATCTC
PDGF-BB	CGAAAGAAGCCCATCTTCAA	AACTTTCGGTGCTTGCCTTT

1.6 Nitric Oxide assay in 264.7 RAW macrophages

RAW cells (100.000 cells/well) were seeded in a 96-wells plate and incubated for 24 hours at 37˚C with 5% CO_2. After 24 hours, RAW medium alone and the conditioned medium of the different treatments of the extracellular FACS-staining of collagen I in 3T3 cells was added to the RAW cells and incubated at 37˚C with 5% CO_2. After 24 hours, 100µl of the supernatant form each well was added to a clear 96-wells plate. Griess reagent was made by adding Griess A (2,003g sulphanilamide + 11,6 ml phosphoric acid 85% supplemented to 200 ml with MilliQ water) to Griess B (200,05mg N-(1-Naphthyl)ethylenediamine dihydrochloride supplemented to 200 ml with MilliQ water) in a 1:1 ratio. The secreted nitrite was measured with the ThermoMax microplate reader (Molecular devices) as absorbance at 550nm. For the calibration curve the $NaNO_2$ 100mM was diluted to concentrations of 0-100µM $NaNO_2$.

1.7 3-[4,5-dimethylthiazole-2-yl]-2,5-diphenyltetrazolium bromide (MTT) assay in 264.7 RAW macrophages

The MTT assay was performed using the same wells plate that was used during the NO assay. 100µl of the samples in the plate was removed and 100µl of Tetrazolium solution (0,5mg/ml in DMEM) was added to each well. The cells were then incubated for 10-60 min at 37˚C. Subsequently, the supernatant was discarded and 100µl of DMSO was added to each well. The plate was then put on a shaker at room temperature until the purple was dissolved after which the absorbance was measured with the ThermoMax microplate reader (Molecular devices) at 550nm.